Quaternary International 384 (2015) 4–12

Contents lists available at ScienceDirect

Quaternary International

journal homepage: www.elsevier.com/locate/quaint

Paleovegetation and paleoclimate changes based on terrestrial *n*-alkanes and their carbon isotopes in sediment from the Jeongok-ri Paleolithic Site, Korea

Sangmin Hyun [a, *], Y.J. Suh [b], K.-H. Shin [c], S.I. Nam [d], Se Won Chang [e], Kidong Bae [f]

[a] Marine Geology and Geophysics Division, Korea Institute of Ocean Science and Technology (KIOST), 787 Hean-ro11, Ansan, 426-744, Republic of Korea
[b] Department of Geology, University of Cincinnati, Cincinnati, OH, 45221, USA
[c] Department of Marine Sciences and Convergent Technology, Hanyang University, Republic of Korea
[d] Korea Polar Research Institute, 26 Songdomirae-ro, Yeonsu-gu, Incheon, 406-840, Republic of Korea
[e] Petroleum and Marine Research Division, Korea Institute of Geoscience and Mineral Resources, Daejeon, 305-350, Republic of Korea
[f] Jeongok Prehistory Museum, Gyeonggi Province, 486-903, Republic of Korea

ARTICLE INFO

Article history:
Available online 7 February 2015

Keywords:
Jeongok-ri
n-alkanes
Carbon isotope
Paleoclimatology
Paleovegetation

ABSTRACT

Carbon isotope of total organic carbon ($\delta^{13}C_{org}$) and long-chain *n*-alkanes, which are terrestrial plant biomarkers, and their compound-specific carbon isotope ratios ($\delta^{13}C_{ALK}$) were investigated in the sediment of the Jeongok-ri Paleolithic Site in central Korea to interpret changes in paleovegetation and paleoclimate. The $\delta^{13}C_{org}$ ranged between approximately −24‰ and −27‰, suggesting different organic matter sources. Relatively lighter $\delta^{13}C_{org}$ occurred in lower part and the occurrence of heavier $\delta^{13}C_{org}$ in upper part may indicate terrestrial C_3 plant dominance and/or a mixture of C_3 and C_4 plants, respectively. The patterns of *n*-alkane distribution were characterized by a continuous predominance of odd-numbered *n*-alkanes, particularly nC_{29} and nC_{31}, and by variation in the distribution of even-numbered *n*-alkanes. Total concentration of *n*-alkanes and distributions of each number of *n*-alkanes are quite different over time, suggesting paleovegetation changes. The average chain length (ACL) and carbon preferences index (CPI) showed gradual variations with distinctive switching points at about 160 ka. This variation reflecting changes in paleovegetation type, is coincident with those of the $\delta^{13}C_{org}$. Individual *n*-alkane isotopes, $\delta^{13}C_{ALK}$, ranged between −18.64‰ and −38.09‰, suggesting different sources of *n*-alkanes. Although some petrogenic sources of *n*-alkanes were possible, the distribution of *n*-alkanes and their $\delta^{13}C_{ALK}$ support paleovegetation and paleoclimatic variations in Jeongok-ri Paleolithic site, Korea for the last 300 ka.

1. Introduction

Records of paleoclimatic variation reveal the alternation of dry and cold climate conditions during glacial periods and warm and humid climate conditions during interglacial periods, particularly in the East Asian monsoon system. These cyclic glacial–interglacial variations are commonly recognized as the dominant geological characteristic during the late Quaternary. Millennial-scale cold and warm climatic signals known as Dansgaard–Oeschger (D-O) cycles, have been clearly demonstrated in marine sediments from East Asian marginal seas (Tada et al., 1999; Nagashima et al., 2011). Cyclic and alternating paleoclimatic and oceanic records can be observed in a wide range of terrestrial and oceanic sediment (Kukla and An, 1989; Rea, 1990; Tada et al., 1999; An, 2000; Lim et al., 2005). As a result, sedimentological and geochemical research has been used to track changes in paleoclimate.

Loess sequences are regarded as an excellent proxy for East Asian monsoon variation, particularly the deposits in inland China (e.g., Xiao et al., 1999; Porter, 2001; Zhang et al., 2006). Dry conditions are generally dominant during glacial periods, causing a large amount of eolian dust and other terrestrial materials to be deposited or transported across the continent to the ocean by strong winds (e.g., Rea, 1990; An, 2000). Glacial and interglacial transport of eolian dust from inland China to the Pacific Ocean and to other land areas has been observed in many areas, demonstrating the alternation of paleoclimatic cycles (e.g., An, 2000; Lee

* Corresponding author.
E-mail address: smhyun@kiost.ac (S. Hyun).

http://dx.doi.org/10.1016/j.quaint.2015.01.012
1040-6182/

et al., 2008; Lim et al., 2013). The variation in the monsoon system provides valuable information regarding local paleoclimatic and vegetation changes, as well as paleoenvironmental changes that are strongly related to human habitation. Therefore the reconstruction of past paleoclimatic variation can be essential for understanding past environmental changes in some areas.

Vegetation changes are often a consequence of climatic changes, as many terrestrial plants are strongly linked to the temperature and humidity of specific environments. Many studies have shown that changes in vegetation are directly associated with changes in local climatic conditions (Takahara et al., 2010; Lim et al., 2013). The impact of this tight association between climatic and vegetation changes may have a global effect (Litwin et al., 2013), perhaps even affecting human life (Alley et al., 2003). In particular, paleovegetation changes has been tracked and interpreted in terms of paleoclimate variation using organic proxy such as *n*-alkanes in various environments (e.g., Yamamoto et al., 2010; Zhang et al., 2010; Zech et al., 2012).

The study area of Jeongok-ri is situated in the central part of the Korean Peninsula and was located in the path of the Asian monsoon winds (westerly jet belt) during the Quaternary (Fig. 1A). Monsoonal patterns may be preserved in the sediment of this area, serving as a record of paleoclimatic variation during the late Quaternary. Additionally, Jeongok-ri is a known site of Paleolithic human habitation (Bae et al., 2001; Shin et al., 2004). These conditions have inspired numerous studies of sediment stratigraphy (Shin et al., 2004), geochronology (Kim et al., 2010), and paleoenvironmental changes (e.g., Kim et al., 2012). However, most of these studies focused on inorganic geochemical changes, and few tested the variability of terrestrial biomarkers. This study used *n*-alkane biomarkers and their compound-specific isotope ratios to reconstruct paleovegetation changes and paleoclimatic variation. Results were compared with those from previous inorganic sedimentary analyses for more precise interpretation.

2. Study site and sampling

The study area is located in the northeastern part of Gyeonggi Province, central Korea (Fig. 1A, B). This site is known for the occurrence of East Asian Acheulian-type stone artifacts (Yi and Clark, 1983). Geologically, Precambrian gneiss is overlain by Jurassic–Cretaceous granite, and an unconsolidated gravel and sand deposit known as the Baekyuri Formation overlies the granite (Lee et al., 1983). Most of the Baekyuri Formation consists of so-called Jeongok basalt. Therefore, the uppermost fine-grained unconsolidated sediment overlies this basalt (Fig. 1C).

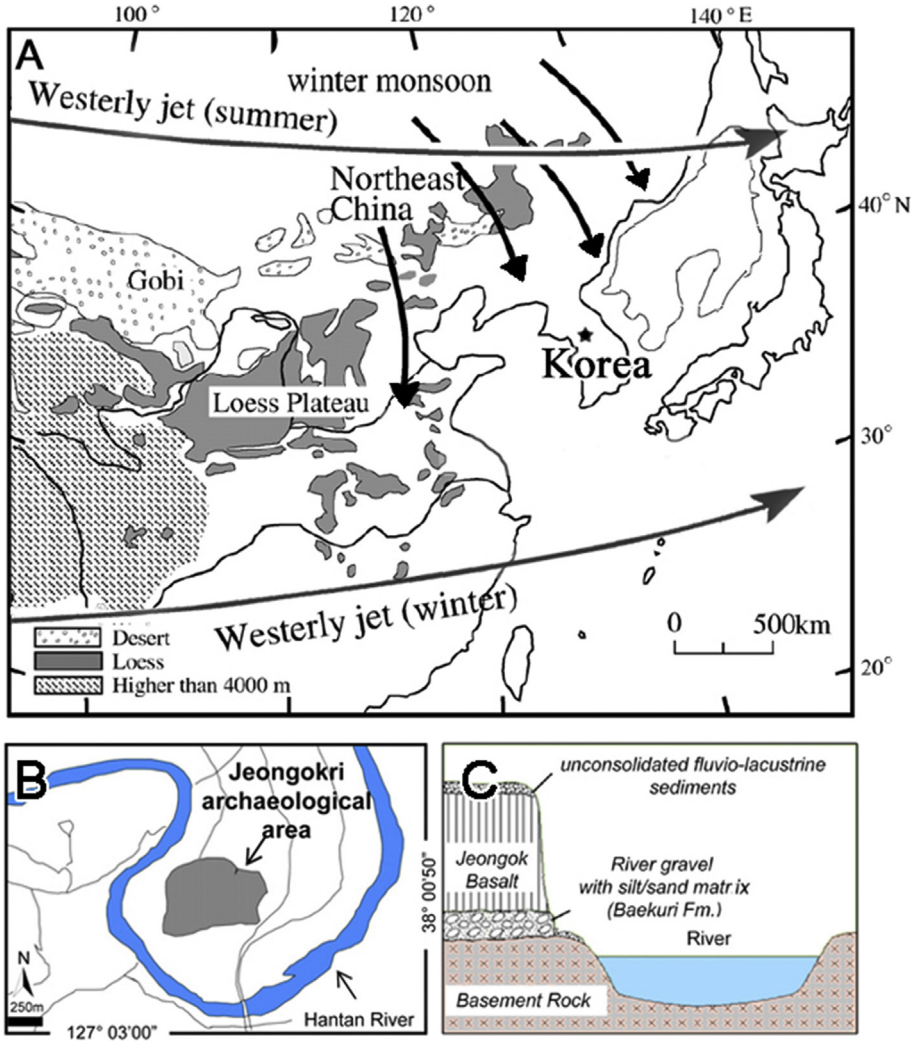

Fig. 1. The Korean peninsula and surrounding area. Schematic representation of monsoon variability (A), the location of the study area, the Jeongok-ri Paleolithic site (B), and vertical view of the site (C). Asterisk indicates the sampling site.

According to Shin et al. (2004), the unconsolidated upper 4 m of this sequence consists of a loess–paleosol deposit, whereas the lower part is composed of fluvial and lacustrine sediment. It has been demonstrated that the upper part of the sediment can be distinguished from the lower part by color changes and geochemical differences (Kim et al., 2012). The geochemical signature of the lower part indicates a highly felsic source rock and suggests that the Hantan River delivered sediment from its catchment area (Fig. 1B). In contrast, increased quartz content and a very fine homogenous grain size in the upper part imply that deposition was associated with eolian processes. A previous study by Kim et al. (2012) showed that the rare earth element (REE) characteristics of the upper part of the sediment were derived from a source with mixed geochemical character, representing the Chinese loess sediments and local sediments from the Korean Peninsula.

In this study, we subsampled for various geochemical analyses from a pre-existing 12-m-long column of sediment, examining a total of 27 samples from the upper 5 m interval. After subsampling, all the samples were dried at 60 °C overnight and crushed by a grinder. The powdered sediment samples were pre-treated in accordance with each analysis.

3. Methods and materials

3.1. Age determination and lithostratigraphy

Many approaches have been used to determine the exact sedimentary age of the Jeongok-ri sediment (Bae et al., 2001; Shin et al., 2004; Kim et al., 2010). The age of the basalt basement is difficult to determine by K–Ar and optically stimulated luminescence (OSL) age dating, with previous studies showing a variety of ages (Table 1). To constrain a more reliable age-depth model, two ^{14}C ages were determined using organic matter from the sediment, and these were compared with previous data. The ^{14}C age samples were collected from sediments at 7.5- and 62-cm depths, and testing was performed by Beta Analytic, Inc. (USA). All the ^{14}C age data and the other measurement results were compared with the previous data and used in this study for a standard lithostratigraphy.

3.2. Organic matter and carbon isotopes

The organic matter content of the Jeongok-ri sediment was measured using a CHNS analyzer (EA1112), and the carbon isotope ratios of the organic matter ($\delta^{13}C_{org}$) were measured using an isotope ratio mass spectrometer (IRMS) (Thermo Fisher Delta 5) at the Korea Polar Research Institute (KOPRI). Total carbon (TC) content was first measured directly without chemical pre-treatment. The total organic carbon (TOC) content was measured after treatment by 1 mol HCL to eliminate inorganic materials at the Korea Institute of Ocean Science and Technology (KIOST). Duplicate analyses revealed high precision, less than about 1% for carbonate and TOC contents, respectively.

Table 1
Age control points mentioned in previous studies (Bae et al., 2001; Kim et al., 2012). Two ^{14}C age dates (based on organic matter) were added in this study.

Depth (cm)	Age (ka)	Methods	Materials	MIS[a]	References
7.5	24.55 ± 120 BP	^{14}C dating	Orgnic matter	2	This study
40	24–25 ka	Tephra	Tephra	2	Yi et al. (1998)
62	34.15 ± 270 BP	^{14}C dating	Orgnic matter	3	This study
90	123	TT-OSL	Sediment	5	Kim et al. (2010)
150	132	OSL	Sediment	6	Kim et al. (2010)
210	135, 137	OSL	Sediment	6	Kim et al. (2010)
270	154, 159	OSL	Sediment	6	Kim et al. (2010)
330	182	OSL	Sediment	7	Kim et al. (2010)
390	200	TT-OSL	Sediment	7	Kim et al. (2010)
Basement	216	Fission track	Basalt	7	Bae et al. (2001)

[a] MIS is marine isotope stage.

3.3. n-alkane analysis

Lipids were extracted over three extraction cycles from dried sediment (about 10 g) using a DIONEX Accelerated Solvent Extractor (ASE 200) at 100 °C and 1500 psi with dichloromethane (DCM)/methanol (MeO)H (95:5). The total lipid extract was concentrated with nitrogen gas using a pressured gas blowing concentrator (D-016, EYELA Tokyo Rikakikai Co.) at KIOST. The extracted lipid was saponified with 1 N KOH/MeOH, and neutral lipid was separated by hexane extraction. The extracted neutral lipid was further separated into four fractions using silica gel column chromatography: F1 (hydrocarbon), F2 (aromatic hydrocarbon), F3 (ketones), and F4 (polar compounds) eluted with hexane (100%), hexane/DCM (2:1, v/v), DCM (100%), and DCM/MeOH (95:5, v/v), respectively.

Gas chromatography (GC) for the analysis of *n*-alkanes in the F1 fraction was conducted using an Hewlett Packard 6890 series GC with a split/splitless injector operated in pulsed splitless mode with electronic pressure control systems and a flame ionization detector (FID). The CP Sil5CB column (60 m × 0.32 mm i.d.) was used with the oven temperature programmed at 50–120 °C at 30 °C/min, at 120–320 °C at 7 °C/min, and then held at 320 °C for 50 min. Prior to quantification of lipids, a known aliquot of an internal standard, 5α-Cholestane (Sigma Aldrich), was added to the hydrocarbon fraction. The compound peak areas were normalized to those of the internal standards and converted to mass quantities using response curves for about 18 hydrocarbon standard compounds (Hydrocarbon Window Defining Standard, AccuStandard) analyzed in concentrations ranging from 10 to 200 μg/ml.

3.4. Carbon isotope of individual n-alkanes ($\delta^{13}C_{ALK}$)

After the *n*-alkane concentration analysis, the fractions were used for the individual *n*-alkane carbon isotope ($\delta^{13}C_{ALK}$) analysis using the GC/IRMS at Hanyang University, Korea. A total of 1 μl of the *n*-alkane concentration was injected into a fused silica capillary column (30 m * 0.32 mm i.d.) for analysis, with helium used as carrier gas. The GC oven temperature was programmed for a stepwise increase from 50 to 310 °C at rates of 30 °C, 6 °C, and 9 °C/min.

All $\delta^{13}C_{ALK}$ values reported in this study were checked for precision and accuracy to interpret small differences in $\delta^{13}C_{ALK}$ values. The standard material (*Methyl heneicosanoate*, $C_{22}H_{44}O_2$) were used and its precisions of $\delta^{13}C_{ALK}$ values from GC/IRMS analyses were reported as the standard deviations (σ) of populations of at least three analyses. The standard deviation of GC/IRMS data for *n*-alkanes was usually less than 0.3‰.

4. Results and discussion

4.1. Comparative lithostratigraphy

The Jeongok-ri sediment column was deposited in the central part of Korea, where Paleolithic remains have been identified. To reconstruct the exact stratigraphy and to evaluate prehistoric environmental changes at this site, a detailed depth *versus* age model was reconstructed using previous age data and newly added ^{14}C ages (Table 1). Previous studies attempting age determination were based on sedimentology, geochemistry, magnetic susceptibility, and inorganic elemental concentrations. These studies determined that the sedimentary column was deposited

successively over the last 300 ka (Bae et al., 2001; Shin et al., 2004; Kim et al., 2010). However, the lower part of the sediment column was regarded as fluvial sediment mixed with a larger grain size. The previous age data obtained by K–Ar, OSL, tephra, and magnetic susceptibility were fundamental for establishing the lithostratigraphy (Kim et al., 2012).

The magnetic susceptibility of this site was examined based on the sedimentary column, revealing a general high intensity in the middle part of the sediment column (Fig. 2). Magnetic susceptibility of the neighboring site in the Dukso area, however, showed high fluctuations similar to the marine isotope stages (MIS) (Yu et al., 2008). Both sites contain similar loess units (units L1LL2, L2, and S2) (Kukla et al., 1988). Given that magnetic susceptibility can be a useful proxy for correct stratigraphy and that the loess units in the two sites are correlative (Meng et al., 1997), our data indicate that the age of the bottom layer of our sedimentary column may correspond to about 300 ka. Age dating by K–Ar and OSL methods revealed a similar age for the bottom layer despite their showing slightly wide range of variability (Table 1).

To determine precise age control, we compared these inorganic data with the MIS SPECMAP curve. The magnetic susceptibility of the sediment column seemed to show a moderate resemblance to that of the nearby Dukso area (located about 50 km away from the study area), and the lithology of the study site and the neighboring site were correlative. Additionally, the magnetic susceptibility of the Dukso site showed moderate correlation with the MIS curve (Yu et al., 2008) (Fig. 2). A comparison of the lithology and stratigraphy of the two sites and the MIS curve showed that the loess-paleosol stratigraphy in the Jeongok-ri sediment column may correlate with the general loess stratigraphy in China and further reflects global-scale MIS variation.

Elements such as Al, Ti, and trace and REEs are regarded as proxies for sediment discrimination (e.g., Yang et al., 2003). Thus, their combination can be useful for sediment provenance determination and as a stratigraphic tool. The major elemental ratio showed a gradual upward variation with reversals at around 240 and 160 ka (Fig. 3). In particular, the vertical profiles of Th, V, and La show similar variations, with reversals at 220, 190, and 160 ka, corresponding to the boundaries of MIS 8/7 and MIS 6. The Th concentration showed an upward decrease at 180 ka, which is roughly coincident with the variation in La and the major elemental ratio. These vertical distributions of major and minor element concentrations imply that different source materials were deposited with a boundary of 160 ka, thus the vertical variation in major and trace elements indicates environmental changes. The magnetic susceptibility showed a significantly different pattern (Fig. 2), and the lithology of the sediment column is highly correlated with the neighboring Dukso area. Therefore, our lithostratigraphy strongly indicates that the sediments in the lower and upper portions of the column at this site are composed of different source materials, with a distinctive geochemical boundary at about 160 ka (Fig. 3).

Based on comparison with previous work and our newly established chronology, the bottom of the sediment was judged to date from approximately 300 ka. Distinctive lithological changes indicate that this sediment column may reflect environmental changes during the past 300 kyr, implying that several

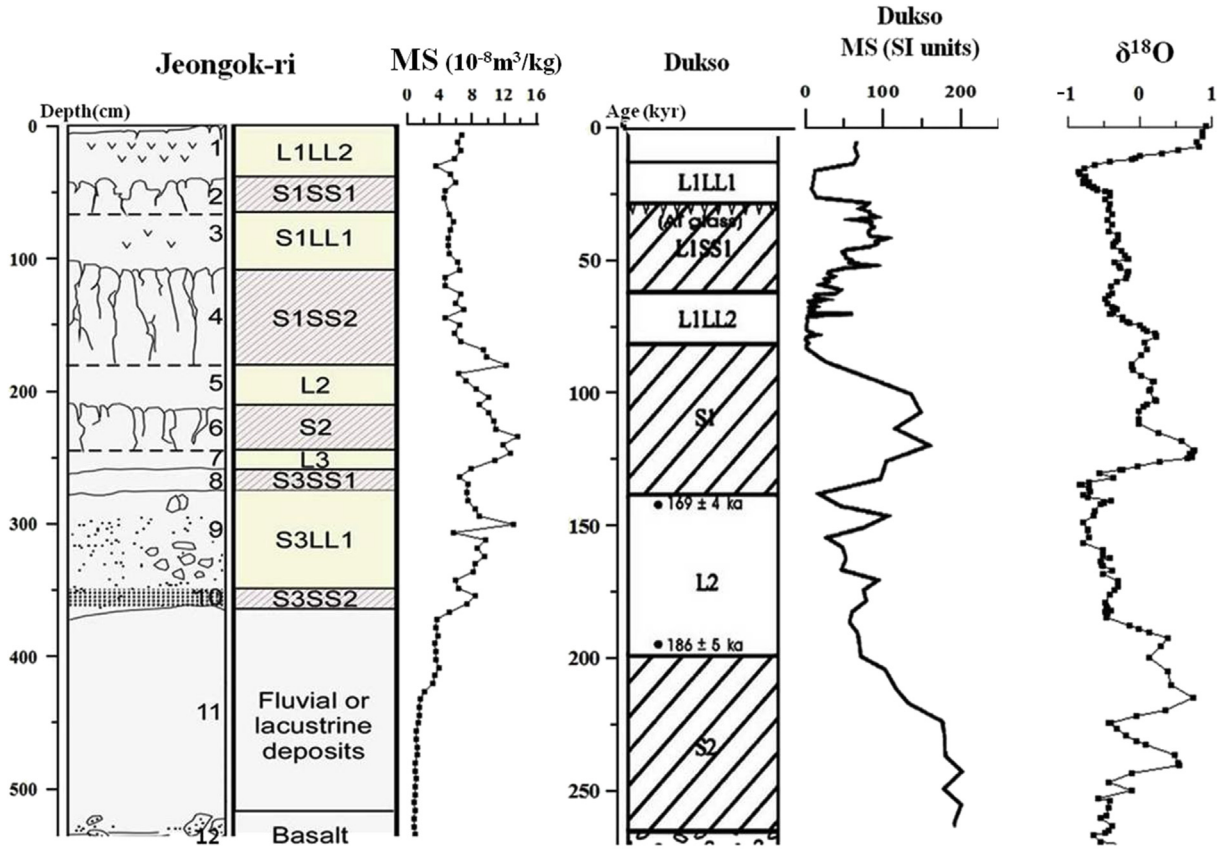

Fig. 2. Stratigraphic column of pit E55S20 (From Bae et al., 2001) with magnetic susceptibility and standard marine isotope stages (MIS) indicated. This pit column section was derived from Bae et al. (2001), modified by Kim et al. (2010), and further modified by the authors. The loess–paleosol units that occurred in both sites were cited from previous work (Yu et al., 2008).

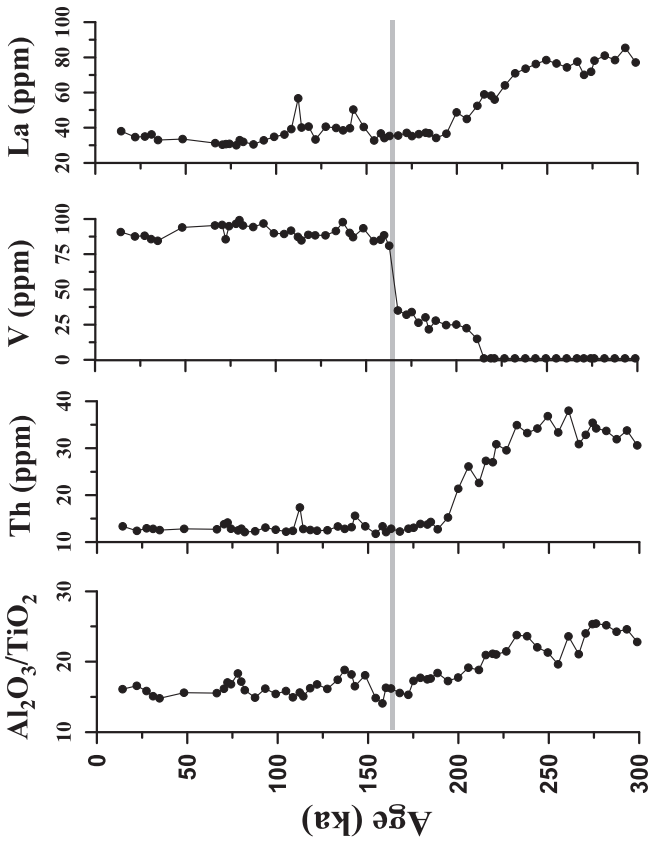

Fig. 3. Vertical variations in Al_2O_3/TiO_2, Th, V, and La in the Jeongok-ri sediments show clear lithological changes, implying gradual changes in the sediment characteristics and sources. All major and trace element data were derived from Kim et al. (2012) and modified in this study. A horizontal bar indicates geochemical boundary.

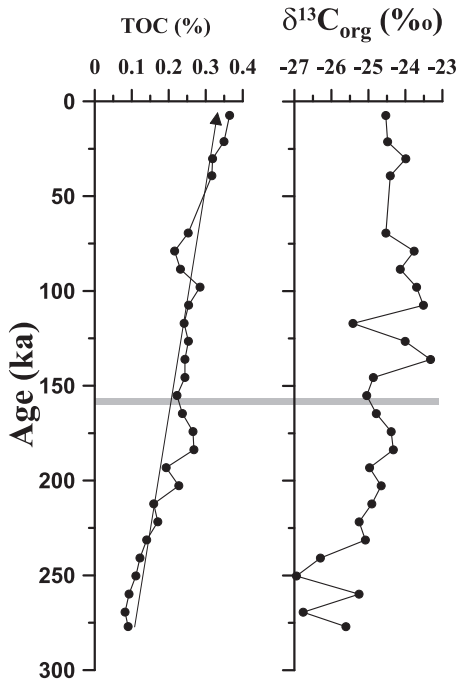

Fig. 4. Vertical profiles of TOC and $\delta^{13}C_{org}$. General upward increases in TOC (%) content and heavier trends in $\delta^{13}C_{org}$ were observed.

glacial–interglacial cycles are recorded in the sediment. The sediment components, including loess, may be evidence of paleoclimatic changes.

4.2. TOC and carbon isotopes of organic matter ($\delta^{13}C_{org}$)

TOC content (%) was relatively low (<0.4%, average: 0.22%, $n = 27$) and generally increased upward, with some decreases between 100 and 75 ka (Fig. 4). TOC content alone does not elucidate the exact source and the pathway even though it has been used widely (e.g., Stein, 1990). Carbon isotopes of organic matter ($\delta^{13}C_{org}$) can provide more reliable information for organic matter source (Minoura et al., 1997) and degradation (Freudenthal et al., 2001), as its value is source dependent. Lighter values of $\delta^{13}C_{org}$ (around −27‰) indicated a terrigenous C_3 plant dominant source, and heavier values of $\delta^{13}C_{org}$ (around −22‰) indicate environments dominated by C_4 plants (Lamb et al., 2006; Lim and Fujiki, 2011).

In our study, $\delta^{13}C_{org}$ values showed a relatively narrow range of variation, between −26.94 and −23.32‰. The excursion of $\delta^{13}C_{org}$ showed an upward heavier trend from about 270 ka to approximately 150 ka and then remained relatively stable with moderate fluctuation (Fig. 4). When previously published end-members were compared with our results, the lightest values in our study reached approximately −27‰, which is the end-member of C_3 plants. Therefore, lighter $\delta^{13}C_{org}$ values in the lower sediments can be interpreted as indicating a dominance of terrigenous C_3 plants. In contrast, the $\delta^{13}C_{org}$ values showed upward heavier trends but did not reach −22‰, the end-member of C_4 plants. This indicates an environment composed of a mixture of C_3 and C_4 plants since ~160 ka.

The variation in $\delta^{13}C_{org}$ can be divided into two stages, with the first stage occurring during approximately 270–160 ka, and the second stage during 160 ka to present (Fig. 4). Before the 160 ka, $\delta^{13}C_{org}$ increased gradually over time from −27 to −24‰ (Fig. 4), indicating an increasing trend of C_4 plants and a decreasing trend of C_3 plants over a 120 ky period. After 160 ka, the values seemed to stabilize at around −23‰, indicating a shift in the environment that may have favored both C_3 and C_4 plant communities.

Assuming that the $\delta^{13}C_{org}$ source for this study area is limited to the terrestrial realm, the amplitude of the $\delta^{13}C_{org}$ variation can be considered either to reflect variation in the surrounding plant community or to represent a long-distance influx of eolian dust from mainland China. The westerly jet means that the material could have originated in the surrounding area or from inland China. The $\delta^{13}C_{org}$ variation showed two stepwise changes indicating paleoclimatic variation; thus, the plant community should have changed in accordance with local environmental changes and paleoclimatic changes. However, it is difficult to determine the degree of transportation of organic materials in this area from $\delta^{13}C_{org}$ variation only. More detailed consideration using the terrestrial biomarker *n*-alkane is discussed in the following section.

4.3. Distribution of terrestrial n-alkane and its implications

As terrestrial biomarkers, long-chain *n*-alkanes are abundant in a variety of environments and are useful for assessing environmental changes. In general, high-molecular-weight *n*-alkanes such as nC_{29} and nC_{31} can originate in typical epicuticular leaf waxes of higher plants, and these biomarkers can easily be transported long distances into the open ocean (Ohkouch et al., 1997; Yokoyama et al., 2006). Usually, *n*-alkanes derived from epicuticular leaf waxes are dominated by long, odd-numbered alkanes within the nC_{24}–nC_{35} range (Eglinton and Eglinton, 2008). In addition, *n*-alkanes from petrogenic sources such as crude oil and high-grade

coal generally show a destruction of the preference for odd carbon numbers with dominance in the nC_{15}–nC_{25} range (Petersen et al., 2007). In this study, the distribution of *n*-alkanes was generally characterized by predominance of odd-numbered *n*-alkanes over even-numbered *n*-alkanes. In particular, high-molecular-weight *n*-alkanes were dominated by nC_{31} and nC_{29} (Fig. 5).

N-alkane predominance can be used to determine the type of higher plant (Sikes et al., 2009; Ahad et al., 2011). In most cases, C_3 plants show a predominance of nC_{29} and nC_{31} *n*-alkanes, and C_4 plants show nC_{33} *n*-alkane predominance. This characteristic distribution of *n*-alkanes is strongly coincident with our *n*-alkene distribution pattern. Therefore, *n*-alkane and $\delta^{13}C_{org}$ variations observed through time support a likely change in source plant type occurring in conjunction with local paleoenvironmental and global paleoclimatic changes.

Average chain length (ACL) provides valuable information about *n*-alkane sources (Jeng, 2006; Bush and Mclnerney, 2013) in particular. ACL values reflect the contribution of petroleum-derived *n*-alkanes in coastal marine sediments *versus* non-contaminated riverine sediments (Jeng, 2006). Therefore, it is possible to delineate the possible *n*-alkane source by identifying environmental differences, even though the usefulness of this approach is constrained to source-specific *n*-alkane distribution only (Jeng, 2006). In present study, the fluctuation in ACL corresponds roughly to the variation in the carbon preference index (CPI) in the upper part of the sediment column (Fig. 6). This pattern can be interpreted as variation in the plant community in whole interval (from 270 ka to present). However, ACL and CPI were relatively constant since 160 ka, suggesting that the majority of plant groups were maintained homogenously. Similar distributions of nC_{29}, nC_{31} and nC_{33} may support an homogenous plant type dominant environment as indicated by ACL and CPI (Fig. 6).

CPI, which is an index of alkanes sources, is known to be higher in terrestrial plant waxes, whereas its value in *n*-alkanes from fossil fuels is relatively lower (Bi et al., 2005). Terrestrial plant waxes generally have high CPI (>3), whereas lower CPI is reflective of short-chain *n*-alkane distribution. This may indicate a contribution from macrophytes, algae, and bacteria (Bi et al., 2005). Therefore, CPI is expressed as a weighted average of the various averages of carbon chain lengths, provides information for source discrimination. In our study, CPI values fluctuated greatly from the base of the sediment to approximately 160 ka, with relatively slight upward increase from 160 ka to present (Fig. 6). However, CPI values generally exceeded 3, indicating that most of *n*-alkane distribution in our study reflected a terrestrial leaf wax source.

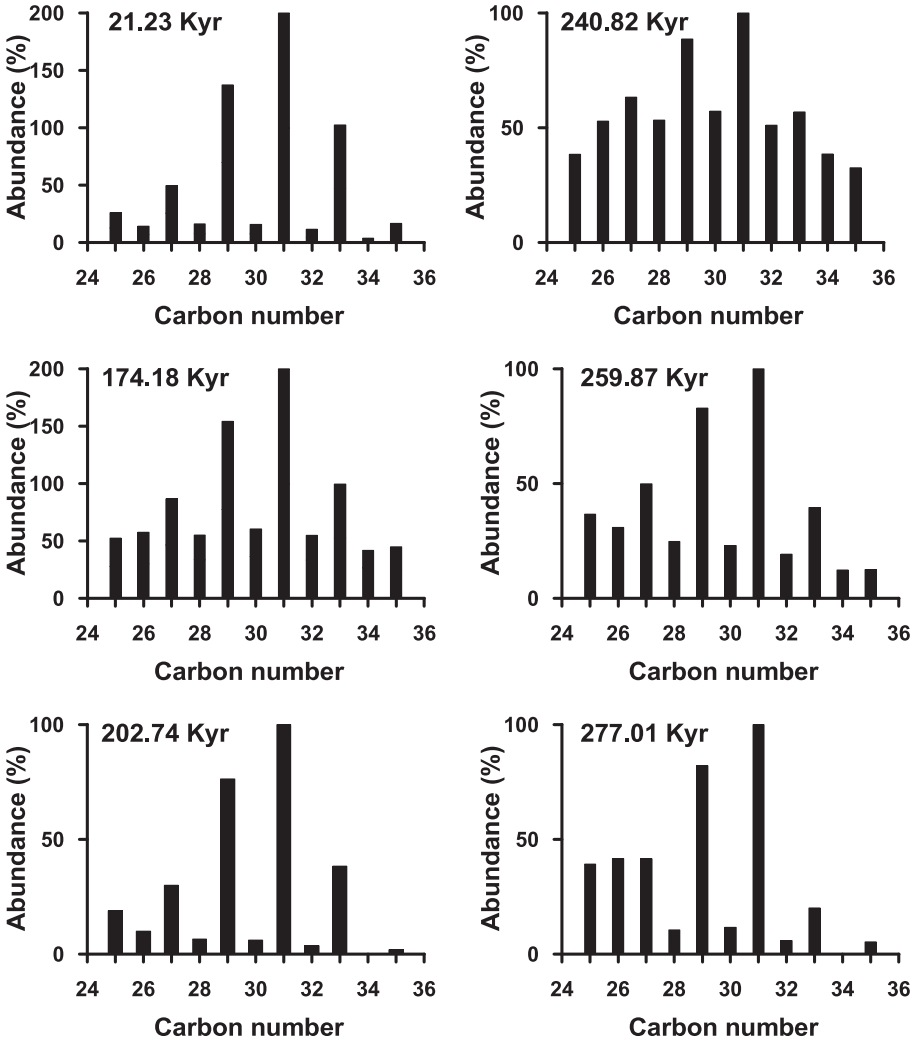

Fig. 5. Distribution of *n*-alkanes. Six representative *n*-alkane distributions are illustrated. The *n*-alkane distribution was clearly differentiated from time to time suggesting paleovegetation changes of surrounding area and/or changes in source area.

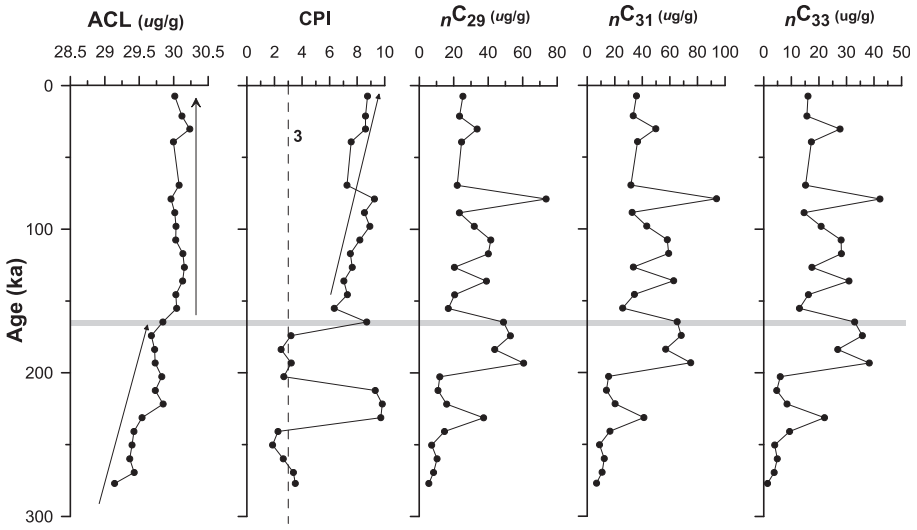

Fig. 6. Average chain length (ACL) and carbon preference index (CPI). Representative odd-numbered *n*-alkanes (nC_{29}, nC_{31}, nC_{33}) are shown. ACL of *n*-alkanes (nC_{25} to nC_{35}) and CPI were calculated by the formula described by Collister et al. (1994). An horizontal bar indicate organic geochemical switching boundary, coincide with TOC (%) and $\delta^{13}C_{org}$ boundaries.

A locally dominant source contributing these two *n*-alkane compounds may be likely because the study area is located in the central part of an inland area. It is possible that these compounds could have been transported from distant terrestrial areas such as inland China, because these compounds can be easily transported from land to the Pacific Ocean (Ohkouch et al., 1997). Additionally, it has been established that large amounts of eolian dust were transported from inland China during late Quaternary (Lim et al., 2005; Lee et al., 2008; Nagashima et al., 2011; Lim et al., 2013). It is difficult to determine the quantity of terrestrial compounds that were transported to our study area. Nevertheless, terrestrial input from other places such as inland China is possible, and this issue is discussed in the following section.

4.4. Individual carbon isotopes of n-alkanes ($\delta^{13}C_{ALK}$) and sources

Investigation of the *n*-alkane compound-specific isotopic ($\delta^{13}C_{ALK}$) ratio has a high potential for complementing *n*-alkane distributions and providing more reliable *n*-alkane provenances (Collister et al., 1994). For this reason, $\delta^{13}C_{ALK}$ has been widely used for *n*-alkane source discrimination because *n*-alkane isotopes show no fractionation during photo oxidation and microbial degradation

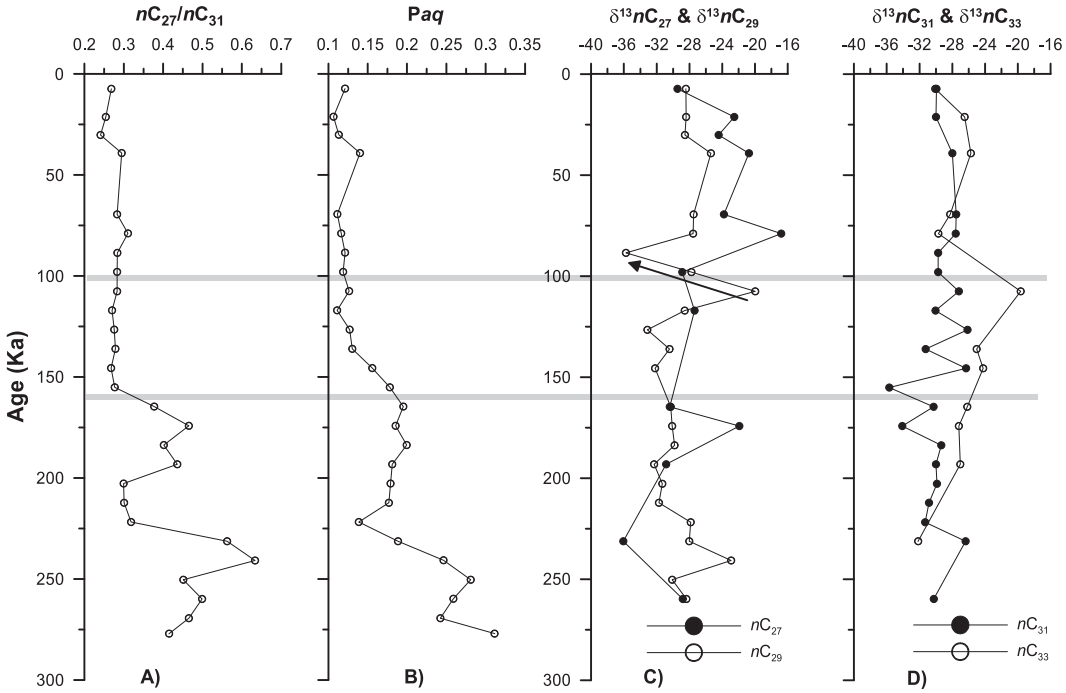

Fig. 7. Vertical profiles of nC_{27}/nC_{31}, P*aq* and individual *n*-alkanes carbon isotope ratios (nC_{27}, nC_{29}, nC_{31} and nC_{33} unit in permil (‰). P*aq* is expressed as $(C_{23} + C_{25})/(C_{23} + C_{25} + C_{29} + C_{31})$ (Yamamoto et al., 2010).

(e.g., Bakel et al., 1994; Ahad et al., 2011). This means that different sources have distinct characteristics for $\delta^{13}C_{ALK}$ values. Previous research showed that $\delta^{13}C_{ALK}$ values for C_4-derived *n*-alkanes were all within the range of −18.5 to −24.5‰, and those for C_3-derived *n*-alkanes were more depleted, ranging from approximately −31.4 to −38.6‰ (Collister et al., 1994).

The entire range of *n*-alkane carbon isotopes of this study varied from −18.64 to −38.09‰, with slightly heavier $\delta^{13}C$ of *n*-alkane values in younger-age intervals. The excursion of $\delta^{13}C_{ALK}$ of nC_{27} and nC_{33} shows upward heavier trend even though they remain stable in uppermost part and since about 100 ka, respectively. However, the excursion of nC_{29} and nC_{31} seems to stable with higher amplitude (Fig. 7). Assuming that the $\delta^{13}C_{ALK}$ values for C_4- and C_3-derived *n*-alkanes were all within the range of −18.5 to −24.5‰ and −31.4 to −38.6‰ is accepted, our wide variability of $\delta^{13}C_{ALK}$ values may imply of mixture of C_4 and C_3-derived *n*-alkanes. For example, nC_{29} showed clear lighting trend within short time period (arrow in Fig. 7) suggesting that major paleovegetation has been shifted from C4 plant to C3 plant at the boundary of 100 ka.

To understand more detailed variations on paleovegetation, we used nC_{27}/nC_{31} and paleoplant proxy (P*aq*), which are used for proxy of paleovegetation changes (Yamamoto et al., 2010). As shown in A) of Fig. 7, distinctive changing boundary was found in nC_{27}/nC_{31} at 160 ka. This excursion shows tight match with carbon isotope of organic matter as shown in Fig. 4. Rather gradual upward variation also recognized in P*aq*. Thus, these two paleovegetation proxies suggest that major plant community has been changed in study area and/or source areas. However, these two paleovegetation proxies do not match with the variation of major $\delta^{13}C_{ALK}$.

Several researchs showed *n*-alkane contamination can be detectable in coastal and estuary sediments (Ishiwatari et al., 1994; Ahad et al., 2011). Ishiwatari et al. (1994) found isotopic difference in odd and even *n*-alkanes (nC_{27}~nC_{33}), and explained higher plant *n*-alkanes mixed with *n*-alkanes from oil pollution in marine sediments by using two end-member mixing models. Also, Ahad et al. (2011) pointed out the possibility of hydrocarbon contamination in estuaries sedimentary environments. However, these samples are likely being undertaken secondary contamination such an environment, and are quite different environment from our study environment. Judging from the $\delta^{13}C_{ALK}$ range in our study, it is hard to account that current $\delta^{13}C_{ALK}$ values were contaminated. Therefore, carbon isotopes of individual *n*-alkanes, particularly $\delta^{13}C_{ALK}$ of nC_{31} and $\delta^{13}C_{ALK}$ of nC_{33}, can provide insight into the source area as well as the changing plant community.

5. Conclusions

Long-chain *n*-alkanes, which are terrestrial plant biomarkers, and their compound-specific carbon isotope ratios ($\delta^{13}C_{ALK}$) were investigated in the sediment of the Jeongok-ri Paleolithic Site in central Korea to interpret changes in paleovegetation and paleoclimate over the last 300 ka. Major changes in *n*-alkane distribution were maintained by a high abundance of three major compounds (nC_{29}, nC_{31}, and nC_{33}), followed by a changing abundance of even-numbered *n*-alkane compounds. This distribution showed repeated characteristics between high abundance of odd-numbered *n*-alkanes with low abundance of even-numbered *n*-alkanes, and high abundance odd-numbered long chain *n*-alkane with relatively high abundance of even-numbered *n*-alkanes. These two distribution patterns are the most distinguishing feature of this study. Therefore, the *n*-alkane distribution may suggest that the vegetation communities varied during the last 300 ka. Furthermore, it implies paleoenvironmental changes in the local forest. Therefore, global climatic variation may have influenced the vegetation community. Compound-specific carbon isotope ratios showed gradual heavier trend in the lower part (270–120 ka) and constant in the upper parts (120 ka ~ present) of the sediment column. Therefore, δ_{13ALK} values reflected the dominant of C_3 plants in lower part of the sediment and the mixture of C_4 and C_3 plants in the upper part. This characteristic observed in individual $\delta^{13}C_{ALK}$ values was confirmed by the variation in $\delta^{13}C_{org}$ values, further indicating that this study area has experienced vegetation changes. Potential glacial–interglacial-scale paleoclimatic variation has influenced the paleovegetation changes of the study area and the East Asian region.

Acknowledgements

This research was part of the project titled “International Ocean Discovery Program (PM58300)” funded by the Ministry of Ocean and Fisheries, Korea. S.I Nam is supported by Basic Research Program (PE15062) of KOPRI. The authors kindly thank the anonymous reviewers. Special thanks are extended to Ms. SJ Kang for drafting the figures and for data arrangement.

References

Ahad, J.M.E., Ganesharm, R.S., Bryant, C.L., Cisneros-Dozal, L.M., Ascough, P.A., Fallick, A.E., Slater, G.F., 2011. Sources of *n*-alkanes in an urbanized estuary: insights from molecular distributions and compound-specific stable and radiocarbon isotopes. Marine Chemistry 126, 239–249.

Alley, R.B., Marotzke, J., Nordhaus, W.D., Overpeck, J.T., Peteet, D.M., Pielke Jr., R.A., Pierrehumbert, R.T., Rhines, P.B., Stocker, T.F., Talley, L.D., Wallace, J.M., 2003. Abrupt climate change. Science 299, 2005–2010.

An, Z.S., 2000. The history and variability of the East Asian paleomonsoon climate. Quaternary Science Reviews 19, 171–187.

Bae, K., Hong, M.Y., Lee, H.Y., Kim, Y.Y., 2001. The Chongok Paleolithic Site, Report of Test-pits Excavation, 2000-2001. The Institute of Cultural Properties, Hanyang University, p. 300 (in Korean).

Bakel, A.J., Ostrom, P.H., Ostrom, N.E., 1994. Carbon isotopic analysis of individual *n*-alkanes: evaluation of accuracy and application to marine particulate organic material. Organic Geochemistry 21, 595–602.

Bi, X., Sheng, G., Liu, X., Li, C., Fu, J., 2005. Molecular and carbon hydrogen isotope composition of *n*-alkanes in plant leaf waxes. Organic Geochemistry 36, 1405–1417.

Bush, R.T., Mclnerney, F.A., 2013. Leaf wax *n*-alkane distributions in and across modern plants: implications for paleoecology and chemotaxonomy. Geochimica et Comochimica Acta 117, 161–179.

Collister, J.W., Rieley, G., Stern, B., Eglinton, G., Fry, B., 1994. Compound-specific $\delta^{13}C$ analyses of leaf lipids from plant with differing carbon dioxide metabolisms. Organic Geochemistry 21, 619–627.

Eglinton, T.L., Eglinton, G., 2008. Molecular proxies for paleoclimatology. Earth and Planetary Science Letters 275, 1–16.

Freudenthal, T., Wagner, T., Wenzhofer, F., Zabel, M., Wefer, G., 2001. Early diagenisis of organic matter from sediments of the eastern subtropical Atlantic: evidence from stable nitrogen and carbon isotopes. Geochimica et Cosmochimica Acta 65, 1795–1808.

Ishiwatari, R., Uzaki, M., Yamada, K., 1994. Carbon isotope composition of individual *n*-alkanes in recent sediments. Organic Geochemistry 21, 801–808.

Jeng, W.-L., 2006. Higher plant *n*-alkanes average chain length as an indicator of petrogenic hydrocarbon contamination in marine sediments. Marine Chemistry 102, 242–251.

Kim, J.C., Duller, G.A.T., Roberts, H.M., Wintle, A.G., Lee, Y.I., Yi, S.B., 2010. Re-evaluation of the chronology of the paleolithic site at Jeongokri, Korea, using OSL and TT-OSL signals from quartz. Quaternary Geochrologoy 5, 365–370.

Kim, J.C., Lee, Y.-I., Lim, H.S., Yi, S., 2012. Geochemistry of Quaternary sediments of the Jeongokri archaeological site, Korea: implications for provenance and paleoenvironments during the Late Pleistocene. Journal of Quaternary Science 27, 260–268.

Kukla, G., An, Z., 1989. Loess stratigraphy in central China. Paleogeography, Paleoclimatology, Paleoecology 72, 203–225.

Kukla, G., Heller, F., Liu, X.M., Xu, T.C., Liu, T.S., An, Z.S., 1988. Pleistocene climates in China dated by magnetic susceptibility. Geology 16, 811–814.

Lamb, A.L., Wilson, G.P., Leng, M.J., 2006. A review of coastal palaeoclimate and relative sea-level reconstructions using $\delta^{13}C$ and C/N ratios in organic material. Earth-Science Reviews 75, 29–57.

Lee, D.S., Ryu, K.J., Kim, G.H., 1983. Geotectonic interpretation of Choogaryong rift Valley, korea. Journal of the Geological Society of Korea 19, 19–38 (in Korean with English abstract).

Lee, S.H., Lee, Y.I., Yoon, H.I., Yoo, K.-C., 2008. East Asian monsoon variation and climate changes in Jeju Island, Korea, during the latest Pleistocene to early Holocene. Quaternary Research 70, 265–274.
Lim, J., Fujiki, T., 2011. Vegetation and climate variability in East Asia driven by low-latitude oceanic forcing during the middle to late Holocene. Quaternary Science Reviews 30, 2487–2497.
Lim, J., Matsumoto, E., Kitagawa, H., 2005. Eolian quartz flux variations in Cheju Island, Korea, during the last 6500 yr and a possible Sun-monsoon linkage. Quaternary Research 64, 12–20.
Lim, J., Kim, J.-Y., Kim, S.-J., Lee, J.-Y., Hong, S.-S., 2013. Late Pleistocene vegetation change in Korea and its possible link to East Asia monsoon and Dansgaard-Oeschger (D-O) cycles. Quaternary Research 79, 55–60.
Litwin, R.J., Smoot, J.P., Pavich, M.J., Markewich, H.W., Brook, G., Durika, N.J., 2013. 100,000-year-long terrestrial record of millennial-scale linkage between eastern North American mid-latitude paleovegetation shifts and Greenland ice-core oxygen isotope trends. Quaternary Research 80, 291–315.
Meng, X., Derbyshire, E., Kemp, R.A., 1997. Origin of the magnetic susceptibility signal in Chinese loess. Quaternary Science Reviews 16, 833–839.
Minoura, K., Hoshino, K., Wada, E., 1997. Late Pleistocene-Holocene paleo-productivity circulation in the Japan Sea: sea-level control on $\delta^{13}C$ and $\delta^{15}N$ records of sediment organic material. Paleogeo Paleoclimatol Paleoecol 135, 41–50.
Nagashima, K., Tada, R., Tani, A., Sun, Y., Isozaki, Y., Toyoda, S., Hasegawa, H., 2011. Millennial-scale oscillations of the westerly jet path during the last glacial period. Journal of Asian Earth Science 40, 1214–1220.
Ohkouch, N., Kawamura, K., Kawahata, H., Taira, A., 1997. Latitudinal distributions of terrestrial biomarkers in the sedimehts from the Central Pacific. Geochimica et Cosmochimica Acta 61, 1911–1918.
Petersen, H.I., Nytoft, H.P., Ratansathien, B., Foopatthankamol, A., 2007. Oils from Cenozoic rift-basins in central and northern Thailand: source and thermal maturity. Journal of Petroleum Geology 30, 59–77.
Porter, S.C., 2001. Chinese loess record of monsoon climate during the last glacial-interglacial cycle. Earth-Science Reviews 54, 115–128.
Rea, D.K., 1990. Aspects of atmospheric circulation: the Late Pleistocene (0-950,000 yr) record of eolian deposition in the Pacific Ocean. Paleogeography, Paleoclimatology, Paleoecology 78, 217–227.
Shin, J.B., Yu, K.M., Naruse, N., Hayashida, A., 2004. Study on loess-paleosol stratigraphy of Quaternary unconsolidated sediments at E55S20 pit of Chongokri Paleolithic Site. Journal of the Geological Society of Korea 40, 369–381 (in Korean with English abstract).
Sikes, E.L., Uhle, M.E., Nodder, S.D., Howard, M.E., 2009. Source of organic matter in a coastal marine environment: evidence from n-alkanes and their $\delta^{13}C$ distributions in the Haurake Gulf, New Zealand. Marine Chemistry 113, 149–163.
Stein, R., 1990. Organic carbon content/sedimentation rate relationship and its paleoenvironmental significance for marine sediments. Geo-Marine Letter 10, 37–44.
Tada, R., Irino, T., Koizumi, I., 1999. Land-ocean linkage over orbital and millennial timescales recorded in late Quaternary sediments of the Japan Sea. Paleoceanography 14, 236–247.
Takahara, H., Igarashi, Y., Hayashi, R., Kumon, F., Liew, P.-M., Yamamoto, M., Kawai, S., Oba, T., Irino, T., 2010. Millennial-scale variability in vegetation records from the East Asian Islands: Taiwan, Japan and Sakhalin. Quaternary Science Reviews 29, 2900–2917.
Xiao, J.L., An, Z.S., Liu, T.S., Inouchi, Y., Kumai, H., Yoshikawa, S., Kondo, Y., 1999. East Asian monsoon variation during the last 130,000 years: evidence from the Loess Plateau of central China and Lake Biwa of Japan. Quaternary Science Reviews 18, 147–157.
Yamamoto, S., Kawamura, K., Seki, O., Meyers, P.A., Zheng, Y., Zhou, W., 2010. Environmental influences over the last 16 ka on compound-specific $\delta^{13}C$ variations of leaf wax n-alkanes in the Hani peat deposit from northeast China. Chemical Geology 277, 261–268.
Yang, S.Y., Jung, H.S., Kim, D.I., Li, C.X., 2003. A review on the provenance discrimination of sediments in the Yellow Sea. Earth-Science Reviews 63, 93–120.
Yi, S., Clark, G.A., 1983. Observation on the lower Paleolithic of Northeast Asia. Current Anthropology 24, 181–202.
Yi, S., Soda, T., Arai, F., 1998. New discovery of Aira-Tn ash (AT) in Korea. Journal of Korean Geographic Society 33, 447–454.
Yokoyama, Y., Naruse, T., Ogawa, N.O., Tada, R., Kitazato, H., Ohkouchi, N., 2006. Dust influx reconstruction during the last 26,000 years inferred from a sedimentary leaf wax record from the Japan Sea. Global and Planetary Change 54, 239–250.
Yu, K.-M., Shin, J.-B., Naruse, T., 2008. Loess-paleosol stratigraphy of dukso area, Namyangju City, korea (South). Quaternary International 176–177, 96–103.
Zech, M., Rass, S., Buggle, B., Loscher, M., Zoller, L., 2012. Reconstruction of the late Quaternary paleoenvironments of the Nussloch loess paleosol sequence, Germany, using *n*-alkane biomarkers. Quaternary Research 78, 226–235.
Zhang, J., Yu, H., Jia, G., Chen, F., Liu, Z., 2010. Terrestrial n-alkane signatures in the middle Okinawa Trough during the past-glacial transgression: control by sea level and paleovegetation confounded by offshore transport. Geo-Marine Letters 30, 143–150.
Zhang, Z., Zhao, M., Egliton, G., Lu, H., Huang, C.-Y., 2006. Leaf wax lipids as paleovegetational and paleoenvironmental proxies for the Chinese Loess Plateau over the last 170 kyr. Quaternary Science Reviews 25, 575–594.